Coupling Between Whistler Waves and Ion-Scale Solitary Waves: Cluster Measurements in the Magnetotail During a Substorm

A. Tenerani,[1,2,*] O. Le Contel,[1] F. Califano,[2] F. Pegoraro,[2] P. Robert,[3] N. Cornilleau-Wehrlin,[3,4] and J. A. Sauvaud[5]

[1]*LPP, CNRS, Ecole Polytechnique, UPMC, St. Maur-des-Fossés 94107, France*

[2]*Physics Department, University of Pisa, Pisa 56127, Italy*

[3]*LPP, CNRS, Ecole Polytechnique, Palaiseau 91128, France*

[4]*LESIA, Observatoire de Paris, Meudon 92195, France*

[5]*IRAP, CNRS, University of Toulouse, Toulouse 31028, France*

(Received 22 March 2012; published 10 October 2012)

We present a new model of self-consistent coupling between low frequency, ion-scale coherent structures with high frequency whistler waves in order to interpret Cluster data. The idea relies on the possibility of trapping whistler waves by inhomogeneous external fields where they can be spatially confined and propagate for times much longer than their characteristic electronic time scale. Here we take the example of a slow magnetosonic soliton acting as a wave guide in analogy with the ducting properties of an inhomogeneous plasma. The soliton is characterized by a magnetic dip and density hump that traps and advects high frequency waves over many ion times. The model represents a new possible way of explaining space measurements often detecting the presence of whistler waves in correspondence to magnetic depressions and density humps. This approach, here given by means of slow solitons, but more general than that, is alternative to the standard approach of considering whistler wave packets as associated with nonpropagating magnetic holes resulting from a mirror-type instability.

DOI: 10.1103/PhysRevLett.109.155005 PACS numbers: 52.65.−y, 52.35.Bj, 52.35.Hr, 52.35.Sb

Whistler mode waves have been extensively studied both in space and laboratory plasmas [1]. It has been shown that whistlers propagating in a cold magnetized plasma can be guided by field aligned tubes of density enhancements or depletions [2–5], the so-called *density ducts*. Thanks to this ducted propagation, which has been confirmed by satellite observations in Earth's magnetosphere [6–8] and in laboratory experiments [9], whistlers are spatially confined and can propagate for times much longer than their typical time scale without being dispersed. In space plasmas, quasi monochromatic whistler waves generated by electron temperature anisotropy, the *lion roars*, are often observed in correspondence to ion-scale magnetic structures. The latter are characterized by magnetic field strength depressions associated with density humps, usually interpreted as nonpropagating mirror modes [10–14]. Mirror modes are the final stage of a mirror instability and as a consequence they need the proper environment conditions in order to develop [15,16]. On the other hand, a variety of nonlinear magnetic waves can naturally arise in collisionless, magnetized plasmas involving both magnetic field and density modulations on the ion-scales, such as oblique Alfvén and slow magnetosonic solitons and solitary kinetic Alfvén waves [17–23]. The interesting question arises of how whistler waves, occurring on the electron scales, can couple to slowly propagating nonlinear waves with typical scale length of the order of the ion-scales, and how these coherent structures come into play as carriers of whistler energy.

We report Cluster spacecraft [24] detection of intense whistler wave packets correlated to coherent ion-scale magnetic structures. Cluster is located in the magnetotail near the magnetic equator at a radial distance of $17R_E$ (Earth's radii) during the substorm event which took place on August 17, 2003 from nearly 16:30 to 17:10 UT. During this time interval the four spacecraft, in tetrahedron configuration, are separated by a distance $d \sim 200$ km, which is less than the typical ion-scale lengths of the magnetotail, namely, the ion gyroradius and the ion inertial length, which are of the order of $\sim$1000 km. At that time Cluster spacecraft were in high telemetry mode, thus giving the possibility of measuring the wave form of the magnetic field perturbations in the whistler frequency range $f_{ci} < f \ll f_{ce}$. During the substorm event, Cluster offers a precious set of data allowing us to inspect dynamics occurring on the electron scales, via whistler waves, and on the ion-scale, simultaneously. In the following, we present an example of a nonlinear, slowly propagating coherent magnetic structure interpreted in terms of a solitary wave on the ion-scale. The soliton, viewed as an inhomogeneous configuration, *quasistatic* on the electron time scale, is able to trap and transport whistler waves in a given frequency range. Our aim is to give a rather simple, but hopefully instructive, alternative with respect to mirror modes, to interpret satellite data of whistler waves correlated to the presence of a magnetic dip and density hump.

For the sake of clarity, the four Cluster satellites will be represented by different colors, namely, C1 black, C2 red, C3 green, and C4 blue. The magnetic field data are

provided by the STAFF and FGM instruments. The STAFF instrument measures the three components of the high frequency fluctuations **b**, up to frequencies $f = 4$ kHz, giving the wave form up to $f = 225$ Hz. The FGM instrument gives the low frequency magnetic field **B**, up to $f \sim 10$ Hz. Ion and electron particle data are measured by CIS-CODIF and PEACE instruments, respectively. The particle distribution moments, such as plasma density, bulk velocity and temperature, are measured with low time resolution (4 s time resolution), but provide nevertheless an estimate of the characteristic plasma parameters. The electric field and the spacecraft potential, used as a proxy for electronic density fluctuations (200 ms time resolution) [25], are measured by the electric field and wave experiment (EFW). On August 17 2003 at 16:30–17:03 UT, when a substorm is taking place, Cluster spacecraft are located in the southern lobe of the magnetotail, near the central current sheet, at about $X_{\mathrm{GSE}} = -17R_E$, $Y_{\mathrm{GSE}} = -6R_E$ and $Z_{\mathrm{GSE}} = 1R_E$ in geocentric solar ecliptic coordinates (GSE: X_{GSE} in the Earth-Sun direction and Y_{GSE} in the ecliptic plane pointing duskward). During the whole period, low and high frequency magnetic and electric field perturbations are detected. A tailward fast flow event is observed between 16:33 and 16:52 UT and an earthward fast flow event between 16:55 and 17:03 UT, during which ions reach velocities up to 1000 km/s. The plasma density oscillates between $n \sim 1$ and $n \sim 0.1$ cm^{-3} (except during a few lobe encounters). During both the tailward and earthward ion flow, events involving the central current sheet traversals have been extensively studied by Refs. [26,27]. Here we focus on one of the most illustrative examples of intense whistler wave packets detected during the substorm correlated to an ion-scale coherent magnetic structure, at 16:57:42–16:57:48 UT, outside the central current sheet. The local mean plasma parameters (averaged over the typical time of the low frequency structure) are the plasma density $n_0 \approx 0.15$ cm^{-3}, the ion and electron temperature $T_i^0 \approx 10$ KeV and $T_e^0 \approx 1$ KeV, respectively, and the electron and ion cyclotron frequency $f_{\mathrm{ce}}^0 \approx 800$ Hz and $f_{\mathrm{ci}}^0 \approx 0.5$ Hz, respectively (in GSE: $B_{0x} = -25$ nT, $B_{0y} = -15$ nT and $B_{0z} = 10$ nT). Ions are flowing earthward at velocity $V_i \approx 500$–600 km/s. Other typical quantities are the Alfvén velocity $V_a \approx 1500$ km/s, the ion sound speed $c_s \approx 1000$ km/s, and the ion and electron plasma beta $\beta_i \approx 0.67$ and $\beta_e \approx 0.067$, respectively. The ion inertial length $d_i \approx 600$ km turns out to be of the same order of the ion gyroradius ρ_i. In Fig. 1 we report Cluster spacecraft measurements between 16:57:36 and 16:57:54 UT. In the first panel we show the modulus of the magnetic field $|\mathbf{B}|$ characterized by a depression of about 25% at around 16:57:45 UT. In panel two, we show the satellite potential fluctuations, i.e., plasma density fluctuations, characterized by an increase of about 50% correlated to the magnetic field depletion. In panels three to six we show the b_z component of the magnetic field in the GSE reference

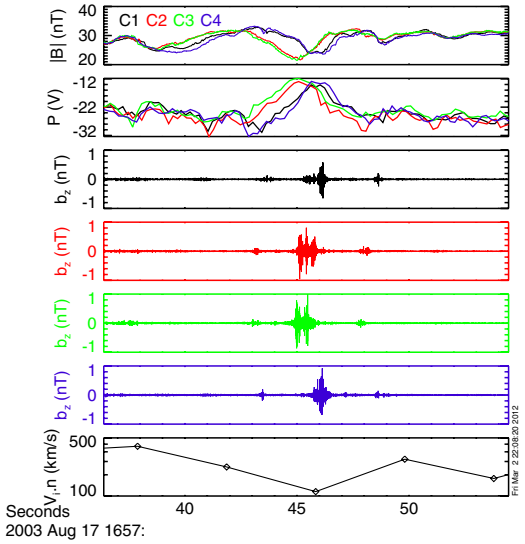

FIG. 1 (color online). First and second panel: the magnitude of the magnetic field $|\mathbf{B}|$ (FGM) and the spacecraft potential (EFW), respectively. Panels three to six: the b_z component in the GSE reference system, C1 to C4, respectively (STAFF-SC). Last panel: the ion velocity measured by C4 parallel to the direction of propagation of the magnetic structure (CIS-CODIF).

system. The last plot represents the ion velocity measured by C4 parallel to the direction of propagation of the coherent, large-scale magnetic structure, as explained below. By means of a polarization analysis carried out for each satellite by using the Means' method [28] (not detailed here) we infer that the high frequency waves are broadband whistlers, unlike lion roars, with frequencies in the range $f = [0.1 - 0.4]f_{\mathrm{ce}}^0$ and that they propagate at an angle $0° < \theta < 30°$ with respect to the background magnetic field. In Fig. 2 we show a zoom of the whistler wave packet (seen by C2). The plots represent the components of the magnetic and electric fields, $\mathbf{b}_{\mathrm{mfa}}$ and $\mathbf{e}_{\mathrm{mfa}}$, perpendicular to the background magnetic field **B**, in black and red color, and the component parallel to **B**, in green. The whistler amplitude is $b/B = 0.05$ and the phase velocity $v_{\mathrm{ph}} \sim e_\perp/b_\perp = 10^4$ km/s. The nature of the low frequency structure has been investigated by using both single and multi-spacecraft techniques of data analysis. From a

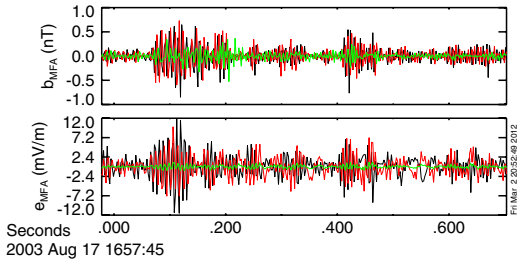

FIG. 2 (color online). The high frequency electric and magnetic fields, $\mathbf{e}_{\mathrm{mfa}}$ and $\mathbf{b}_{\mathrm{mfa}}$, in the magnetic field aligned reference system for C2 (STAFF-SC and EFW).

multi-spacecraft analysis, by assuming the large scale structure as one dimensional and moving through satellites without changing its direction, it is possible to obtain the velocity of propagation v_0 of the structure itself with respect to Cluster satellites and the gradient direction of the magnetic structure, i.e., the normal $\mathbf{n}$ [29,30]. For a plane wave, as our structure will be considered, the normal is directed along the wave vector $\mathbf{k}$. This velocity turns out to be $v_0 = 174 \pm 16\,\mathrm{km/s}$ directed almost in the $\{X_{\mathrm{GSE}} - Y_{\mathrm{GSE}}\}$ direction ($\mathbf{n} = \{0.5, -0.8, -0.4\} \pm 0.1$ in GSE) and quasi perpendicular to the mean magnetic field. Furthermore, each satellite detects the magnetic structure during a time interval lasting about $\Delta T = 5$ s, so that we estimate a typical width of the structure $\ell \approx 900$ km $\lesssim 2\rho_i$. The inferred normal is in agreement with the results obtained from the minimum variance analysis (MVA) [31] that we performed on each satellite. The direction z_{mva} of the minimum variance component, which is a proxy for the normal of the magnetic structure, is almost along $\mathbf{n}$ (for C4 $z_{\mathrm{MVA}} = \{0.5, -0.9, -0.2\}$ in GSE, eigenvalues: $\lambda_{\mathrm{max}} = 0.05$, $\lambda_{\mathrm{int}} = 0.01$, $\lambda_{\mathrm{min}} = 0.0004$). MVA results show a well-defined minimum variance direction; thus, the nonlinear wave is to a good approximation of a 1D structure. As a first approximation, we can assume a nonlinear plane wave. For the sake of clarity, hereafter we will not distinguish between the normal and the minimum variance direction of the structure. In Fig. 3, on the left-hand side, we show the low frequency magnetic field perturbation $\delta\mathbf{B}/B_0 = (\mathbf{B} - \mathbf{B}_0)/B_0$ for the four spacecraft in the MVA coordinate system of C4. The normalized maximum, intermediate, and minimum variance components are represented in the first, second and third panel, respectively. In panels four and five we show the raw data of the electric field averaged over 0.04 s for C2 and C4, respectively, in the MVA system of C4. The raw electric field is measured approximatively along the X_{GSE} and Y_{GSE} directions only, so we imposed the third electric field component equal to zero. We nevertheless point out that the normal direction is mainly along the X_{GSE} and Y_{GSE} directions, so that we expect to find a good description of the electric field of the low frequency structure along the normal direction (green color). In Fig. 3, on the right-hand side, we show the magnetic hodograph for C4 in the plane $\{\delta B_{\mathrm{max}}/B_0, \delta B_{\mathrm{min}}/B_0\}$. The normal direction points inward the page, so that the low frequency wave is elliptically left-handed polarized in the rest frame of the satellites. The electromagnetic structure is characterized by a strong shear component, corresponding to the maximum variance component (Fig. 3, first panel on the left) and a small compressional component, corresponding to the intermediate variance component (Fig. 3, second panel on the left). The electric field along $\mathbf{n}$, the green line in panels four and five of Fig. 3, is in antiphase with the magnetic field as expected for a highly oblique wave. In order to distinguish between a propagating nonlinear wave or a purely advected coherent structure, as it would be for a mirror mode, we have compared the ion velocity projected along the normal $V_{i,n} = \mathbf{V}_i \cdot \mathbf{n}$, and the velocity of propagation v_0 of the magnetic structure. The ion velocity $V_{i,n}$ is represented in the last panel of Fig. 1. Even if time resolution is not appropriate to compare the ion and the magnetic structure velocities accurately, we remark that outside the low frequency structure, where the medium is more stable over the spin period of the satellites and then the particle measurements are well defined, the ion velocity is $V_{i,n} \approx 400 \pm 100$ km/s. This velocity is greater than that of the structure, $v_0 \sim 174 \pm 16$ km/s, thus giving the velocity of propagation of the low frequency wave in the plasma rest frame $V = v_0 - V_{i,n} \approx -225 \pm 116$ km/s, much less than the ion sound speed. The change in the direction of propagation implies that the wave is right handed polarized in the plasma rest frame. We finally underline that from particle temperatures (not shown here), the ion temperature anisotropy is well below the threshold for the onset of the mirror instability [15].

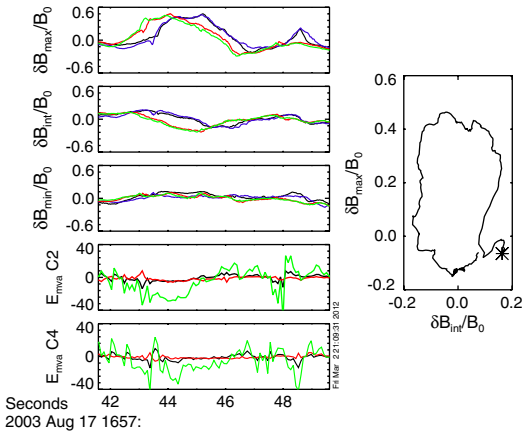

FIG. 3 (color online). Left: Magnetic (FGM) and electric (EFW) fields in the MVA coordinate system of C4. First, second, and third panels represent the normalized maximum, intermediate and minimum variance component, respectively, of the magnetic field. Panels four and five represent the raw data of the electric field (in mV/m) for C2 and C4, respectively. Green (lighter grey), red (darker grey), and black colors correspond to the minimum, intermediate, and maximum variance directions, respectively. Right: magnetic hodograph for C4.

A detailed analysis of the low frequency structure shows that it can be modeled as a nonlinear coherent wave, a solitary wave or soliton, propagating at subsonic speed in a direction quasi perpendicular to the magnetic field. The typical scale is of the order of the ion-scales d_i and ρ_i. The strong shear component of the magnetic field perturbation and the ordering $k_\perp \rho_i \sim 1$ suggest that the low frequency wave is a type of solitary kinetic Alfvén wave. It is known that shear Alfvén waves become dispersive and change to kinetic Alfvén waves when the ion gyroradius is of the order of the perpendicular wave length. If the plasma beta is of order unity, as it is in our conditions, the effect of

plasma compressibility can no longer be neglected. This leads to the coupling of the shear branch with the slow branch, so that compressions of plasma density are associated with magnetic rarefactions [32], and it is found that the kinetic Alfvén wave is right-hand polarized. The correlation of density hump to magnetic field strength minimum is crucial in order to have ducted propagation of whistler waves, which can be channeled by plasma inhomogeneities perpendicular to the magnetic field. In particular, whistlers can be channeled by density humps associated with magnetic field minima for frequencies $f/f_{ce}^{in} < 1/2$, where f_{ce}^{in} is the electron cyclotron frequency at the center of the magnetic depression. The density hump associated with a magnetic field minimum leads to stronger gradients in the refractive index with respect to simple density ducts, thus yielding less strict conditions on the maximum propagation angle for trapped whistlers ([33] and references therein). When the inhomogeneity is provided by a solitary wave, the latter interacts with whistlers by acting as a wave carrier, thus confining and transporting the whistler energy, as distinguished from flux-frozen magnetic structures acting instead as passive channels for whistlers. The mechanism of whistler confinement and transport relies on the shape of the inhomogeneity, which must have a magnetic field minimum associated with a density hump quasi perpendicular to the mean magnetic field, and on the slow propagation velocity of the inhomogeneity with respect to the whistler phase velocity. In this way the soliton can be considered as a local channel for whistlers but *slowly* propagating. Even if a fully nonlinear kinetic treatment should be necessary, as a first step we have investigated the trapping and transport of whistler waves, in the regime of frequencies $f/f_{ce}^{in} < 1/2$, by an ion-scale soliton in the framework of a two-fluid description. In particular, we modeled the soliton by a magnetosonic slow soliton, which, despite lacking the strong shear component, is characterized by a magnetic field strength minimum and a density hump and propagates at a subsonic speed, quasi perpendicular to the background magnetic field. In addition to magnetosonic slow solitons, other solitary waves showing similar features could in principle act as whistler wave carriers (not discussed here). In order to catch the basic physics of the interaction between slow solitary waves and whistlers we have employed a two-fluid numerical code. It has been shown that a two-fluid model can be reduced to a Korteweg de Vries equation in the weakly nonlinear approximation, describing slow and fast oblique magnetosonic solitons [17]. As an initial condition, we have adopted the analytical solution corresponding to a slow magnetosonic soliton profile; see plots in Fig. 4, right panel. Whistlers with chosen frequency and propagation angle are initially injected inside the soliton, at the center of the simulation domain, by a forcing current oscillating at frequency f_0, normalized to the ion cyclotron frequency. The forcing switches off after a few whistler periods. The

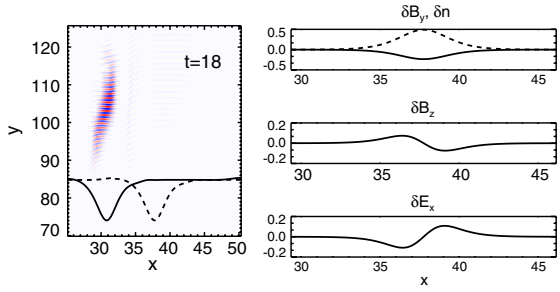

FIG. 4 (color online). Simulation results. Left: detail of the shaded contours of the b_x component of the whistler magnetic field at time $t = 18\omega_{ci}$. The profile of the soliton is represented by the black lines. The dashed line represents the soliton at time $t = 0$. Right: density perturbation and compressional perturbation in the magnetic field (dashed and solid lines, first panel), magnetic field shear perturbation (second panel) and electric field along the normal direction (last panel) of the magnetosonic soliton.

complete analysis, including a WKB study, on the conditions for whistler trapping by a slow soliton is reported in Ref. [33]. Here we limit ourselves to a case example of a simulation where the soliton propagates at an angle $\alpha_0 = 80°$ with respect to the asymptotic magnetic field, with typical width $\ell \sim 4d_i$. The soliton moves in the positive x direction (that is analogous to the normal direction $\mathbf{n}$) but is advected by a background ion flow in the opposite direction. Due to the presence of the soliton, the density increases to $\delta n/n_0 \sim 0.5$ and the magnetic field decreases to $\delta B/B_0 \sim -0.25$. The plasma beta outside the soliton is $\beta_i = \beta_e = 0.3$. The sound speed and propagation velocity, normalized to the asymptotic Alfvén velocity, are $c_s = 0.7$ and $V \sim 0.1$, respectively, to be compared to the whistler wave phase speed which is greater than unity. The whistlers are injected inside the soliton at frequency $f_0/f_{ce}^{in} \sim 0.2$ in the y direction, which is nearly parallel to the background magnetic field. Results are shown in Fig. 4, left panel, where we show a zoom around the soliton of the shaded contours of the x component of the whistler magnetic field b_x at $t = 18\omega_{ci}$. The profile of the soliton is represented (not in scale) by black lines and the dashed line corresponds to the soliton at $t = 0$. Simulation results clearly show that the whistler wave packet, while propagating, is confined and advected by the soliton in its direction of propagation.

Our data show that whistlers are correlated to plasma density and magnetic field strength modulations that show signatures of a subsonic nonlinear wave. Thanks to the compressional component of the solitary wave, which leads to a magnetic field strength minimum in opposition of phase to the plasma density modulation, whistlers can be spatially confined and transported across magnetic field lines by the nonlinear wave itself (the carrier wave). Simulation results, where for simplicity we used as a theoretical model for the carrier wave a slow magnetosonic soliton, show that whistlers are efficiently trapped.

For the first time we report in this Letter an example of whistler ducted propagation in the magnetotail during a substorm. It is worth noting that this mechanism can play an important role in global processes that take place during substorms, such as energy transport and dissipation. Indeed, the nonlinear wave, moving azimuthally to the tail's magnetic field, can extract a significant amount of energy from earthward fast plasma flows which develop during substorms and can contribute to the braking of the flow itself [34]. Furthermore, thanks to the spatial confinement by the nonlinear wave, whistlers can provide strong electron pitch-angle scattering, since the diffusion coefficient scales with the whistler intensity [35]. Thus electrons can be diffused into the loss cone and can be lost when they precipitate into the ionosphere, where their energy is dissipated. Finally, we remark that the fact that all satellites detect the trapped whistlers while the confining structure propagates suggests that the source is either correlated with the structure itself or al least is active for a time long on the structure transit time. A deeper investigation of the whistler source is still an open issue, as well as an inspection of kinetic effects on Alfvénic solitary waves.

We are pleased to acknowledge the Cluster Active Archive and PIs for providing the experimental data and the CINECA super computing center (Italy) where part of the simulations were performed. A. Tenerani wishes to acknowledge O. Alexandrova for useful discussions.

*anna.tenerani@lpp.polytechnique.fr

[1] R. L. Stenzel, J. Geophys. Res. **104**, 14 379 (1999).
[2] R. L. Smith, R. A. Helliwell, and I. W. Yabroff, J. Geophys. Res. **65**, 815 (1960).
[3] V. I. Karpman and R. N. Kaufman, Sov. Phys. JETP **53**, 956 (1981).
[4] V. I. Karpman and R. N. Kaufman, J. Plasma Phys. **27**, 225 (1982).
[5] A. V. Streltsov, M. Lampe, W. Manheimer, G. Ganguli, and G. Joyce, J. Geophys. Res. **111**, A03 216 (2006).
[6] J. J. Angerami, J. Geophys. Res. **75**, 6115 (1970).
[7] H. C. Koons, J. Geophys. Res. **94**, 15 393 (1989).
[8] O. Moullard, A. Masson, H. Laakso, M. Parrot, P. Décréau, O. Santolik, and M. Andre, Geophys. Res. Lett. **29**, 1975 (2002).
[9] R. L. Stenzel, Geophys. Res. Lett. **3**, 61 (1976).
[10] E. M. Dubinin *et al.*, Ann. Geophys. **25**, 303 (2007).
[11] E. J. Smith and B. T. Tsurutani, J. Geophys. Res. **81**, 2261 (1976).
[12] R. M. Thorne and B. T. Tsurutani, Nature (London) **293**, 384 (1981).
[13] B. T. Tsurutani, E. J. Smith, R. R. Anderson, K. W. Ogilvie, J. D. Scudder, D. N. Baker, and S. J. Bame, J. Geophys. Res. **87**, 6060 (1982).
[14] W. Baumjohann, R. A. Treumann, E. Georgescu, G. Haerendel, K.-H. Fornacon, and U. Auster, Ann. Geophys. **17**, 1528 (1999).
[15] D. J. Southwood and M. G. Kivelson, J. Geophys. Res. **98**, 9181 (1993).
[16] M. G. Kivelson and D. J. Southwood, J. Geophys. Res. **101**, 17 365 (1996).
[17] Y. Ohsawa, Phys. Fluids **29**, 1844 (1986).
[18] K. Baumgartel, J. Geophys. Res. **104**, 28 295 (1999).
[19] J. F. McKenzie and T. B. Doyle, Phys. Plasmas **9**, 55 (2002).
[20] K. Stasiewicz, P. Shukla, G. Gustafsson, S. Buchert, B. Lavraud, B. Thidé, and Z. Klos, Phys. Rev. Lett. **90**, 085002 (2003).
[21] K. Stasiewicz, Phys. Rev. Lett. **93**, 125004 (2004).
[22] K. Stasiewicz, J. Geophys. Res. **110**, A03 220 (2005).
[23] D. J. Wu, G. L. Huang, D. Y. Wang, and C. G. Fälthammar, Phys. Plasmas **3**, 2879 (1996).
[24] *The Cluster and Phoenix Missions* edited by C. P. Escoubet, C. T. Russel, and R. Schmidt (Kluwer Academic, Dordrecht, 1997).
[25] A. Pedersen, P. Décréau, C.-P. Escoubet, G. Gustafsson, H. Laakso, P.-A. Lindqvist, B. Lybekk, A. Masson, F. Mozer, and A. Vaivads, Ann. Geophys. **19**, 1483 (2001).
[26] R. Nakamura *et al.*, J. Geophys. Res. **113**, A07 S16 (2008).
[27] P. D. Henderson, C. J. Owen, A. D. Lahiff, I. V. Alexeev, A. N. Fazakerley, E. Lucek, and H. Rème, Geophys. Res. Lett. **33**, L22 106 (2006).
[28] J. D. Means, J. Geophys. Res. **77**, 5551 (1972).
[29] N. Cornilleau-Wehrlin *et al.*, Ann. Geophys. **21**, 437 (2003).
[30] J. Vogt, G. Paschmann, and G. Chanteur, *Reciprocal Vectors, in Multi-Spacecraft Analysis Methods Revisited*, edited by G. Paschmann and P. W. Daly, ISSI SR-008 (ESA Publication Division, Noordwijk, The Netherlands, 2008), p. 33.
[31] B. Sonnerup and M. Scheible, *Minimum and Maximum Variance Analysis, in Analysis Methods for Multi-Spacecraft Data*, edited by G. Paschmann and P. Daly, ISSI SR-001 (ESA Publication Division, Noordwijk, The Netherlands, 1998), p. 185.
[32] J. V. Hollweg, J. Geophys. Res. **104**, 14 811 (1999).
[33] A. Tenerani, F. Califano, F. Pegoraro, and O. Le Contel, Phys. Plasmas **19**, 052 103 (2012).
[34] V. Angelopoulos, J. A. Chapman, F. S. Mozer, J. D. Scudder, C. T. Russell, K. Tsuruda, T. Mukai, T. J. Hughes, and K. Yumoto, J. Geophys. Res. **107**, 1181 (2002).
[35] C. F. Kennel and H. E. Petschek, J. Geophys. Res. **71**, 1 (1966).